CDF/DOC/EXOTIC/CDFR/9375
version 1.04 June 30, 2008

Cross-checks of the CDF-9230

M.Herndon(University of Wisconsin, Madison), P.Murat(Fermilab)

Abstract

In this note we present independent cross-checks of the results described in CDF-9230[1]. We find that

- muon tracks with silicon hits and large impact parameters have their silicon hits misassigned, so large impact parameters of these tracks are not confirmed by the SVX;
- long tails in the distributions in muon track impact parameter are not unique to the muon sample of CDF-9230. Similar tails are also observed in other data samples including JET20 tracks, which makes exotic origin of the tails unlikely;
- distributions in muon ID variables for muons from CDF-9230 analysis sample are consistent with these muons being predominantly fakes.
- analysis sample of CDF-9230 is dominated by high-Et dijet events. Average number of muons per jet of given E_T, $\bar{N}_\mu(E_T)$, measured in the analysis sample, is consistent with measurements of $\bar{N}_\mu(E_T)$ in generic QCD samples.

In conclusion, we find that effects observed in CDF-9230 can be explained by the detector and reconstruction effects and that all the distributions we have studied are consistent with the analysis sample of CDF-9230 being dominated by QCD events with the fake muons reconstructed inside the jets.

We explain how the background subtraction procedure used in CDF-9230 could result in a sample enriched with such events.

Contents

1 Introduction

CDF-9230 reports an observation of 2 interesting features of events taken with dimuon trigger in $p\bar{p}$ interactions:

- an anomalously high rate of multi-muon events
- an anomalously large number of muons which tracks have SVX hits and very large (gt 0.5 cm) impact parameter

In this note we perfrom independent cross-checks of these results. Material in the following sections is organized as follows:

- Section 2 describes the data samples used;
- Section 3 reports results of the tracking studies;
- In Section 4 we study muons in the multi-muon events of CDF-9230 analysis sample;
- In Section 5 we compare jets reconstructed in the CDF-9230 analysis sample to the JET70 and JET100 jets and measure $\bar{N}_\mu(E_T)$ - average number of muons reconstructed within a jet as a function of jet E_T.

CDF-9230 uses rather loose cuts to identify analysis objects which may create difficulties in controlling the fake background.

- to be considered as a "silicon track", a track is required to have 3 or more axial hits in the silicon detector.
- muons used in the analysis CDF-9230 are selected only by P_T-independent cuts on track-to-stub residuals: $\mid \Delta X_{\rm CMU} \mid \; < \;$ 20cm, $\mid \Delta X_{\rm CMP} \mid \; < \;$ 40cm, no other muon identification cuts are applied.

and cross-checks described in this note are therefore focused on understanding purity and composition of the data sample analysed there.

2 Data Samples

Analysis sample of CDF-9230 includes events taken with dimuon trigger which in addition to 2 trigger CMUP muons have additional muons within cone of $cos\theta > 0.8$ from the trigger ones.

Cross-checks performed in this note use the following data samples.

- a subset of 7494 events from CDF-9230 analysis sample, kindly provided by its authors. This subset includes all events with at least one additional muon within cone of $cos\theta = 0.8$ around each of the 2 trigger muons, such that each event has at least 4 reconstructed muons.

  Events have been stripped from jmbb* DST's and STNTUPLE jmbba* datasets. This sample, a relatively small but potentially the most interesting part of the CDF-9230 analysis sample, in the following sections is referred to as GHOST22 sample

- for comparisons we use data samples taken with inclusive 20 GeV, 50 GeV, 70 GeV and 100 GeV jet triggers (JET20, JET50, JET70 and JET100 datasets respectively). These datasets are dominated by the QCD events and are not expected to contain any significant fraction of exotic events.

- we also use sample of J/psi events **JPSI sample: Matt**

3 Cross Checks of the Track Reconstruction

First observation made in CDF-9230 is observation of the muons which tracks have silicon hits and anomalously large impact parameters. We start from understanding quality of these tracks.

3.1 SVX tracking

Loose SVX selection of CDF-9230 which requires a track to have at least 3 axial silicon hits. To check quality of the SVX hit assignment we split all the tracks of CMUP muons reconstructed in GHOST22 sample into 2 categories

- **prompt tracks** : tracks with impact parameter $\mid D0 \mid < 5$mm;
- **displaced tracks**: tracks with $\mid D0 \mid > 5$mm.

and compare them to tracks of the CMUP muons reconstructed in JET50 sample. Fig. 1 compares distributions for the number of different types of SVX hits found on a track. Comparisons for prompt and displaced tracks are shown separately.

Distributions for the number of hits on prompt tracks for JET50 and GHOST22 samples are very similar modulo difference in the instantaneous luminosities, which results in the larger fraction of tracks w/o the silicon hits in GHOST22 sample.

Distributions for the number of hits on displaced tracks for JET50 and GHOST22 samples are also very similar, however, in contrast with the prompts tracks, displaced tracks, in both GHOST22 and JET50 samples, have significantly lower number of silicon hits. About 80% of displaced tracks in GHOST22 sample do not have SVX hits at all, corresponding number for the prompt tracks is significantly lower - about 11%.

An important measure of track quality is the χ^2 of the track fit. Fig. 2 compares distributions in χ^2_{SVX} for prompt and displaced CMUP muon tracks in GHOST22 and JET50 samples. χ^2_{SVX} distributions for tracks with different - 3, 4, and 5 - number axial silicon hits are shown separately.

χ^2_{SVX} distributions for both samples are very similar, the displaced tracks have significantly larger values of χ^2_{SVX} than the prompt tracks. Combined with the significantly smaller number of hits on displaced tracks, this points towards hit misassignment.

We now introduce 2 variables, sensitive to the quality of silicon hits assignment to a track. For a track with the innermost hit found in SVX layer number **i** one can calculate $P_{ax}(j)$ - a probability to find an axial SVX hit in a layer **j** , where j > i.

Distributions in $P_{ax}(j)$ for prompt and displaced tracks are shown in 2 top plots in Fig. 3 and one can see that the distributions for JET50 and GHOST22 samples are very close to each other while distributions for the prompt and displaced tracks in both samples are very different. For a prompt track typical value of $P_{ax}(j)$ is about 0.7-0.9, while for displaced tracks $P_{ax}(j)$ is about 1.5-2 times lower. Assuming an innermost silicon hit is assigned to a track correctly, probability to find a hit in any outer silicon layer should not depend on position of the muon production vertex.

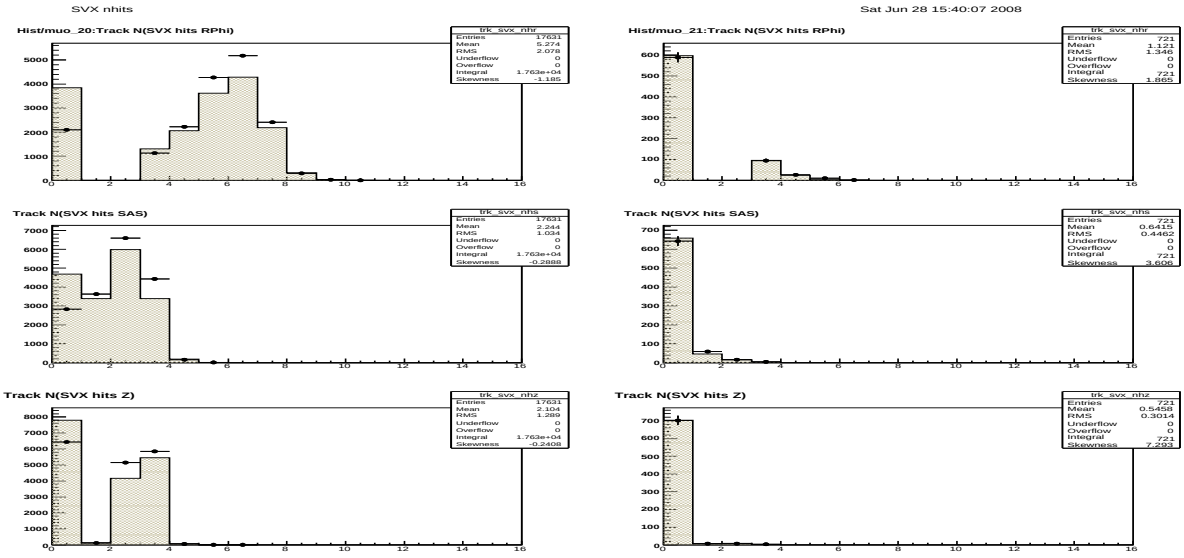

Figure 1: Distributions for number of silicon hits on a track. Left: prompt tracks, right - displaced tracks. Points: GHOST22 sample, histograms: JET50.

Big difference between the prompt and displaced tracks can only be explained by that the displaced tracks often have their innermost hit, as well as the rest ones, misassigned.

Finally, given an axial hit found on a track, one can expect a probability to find a stereo hit (SAS or RZ) in the same layer to depend only on the readout geometry but not on the position of a particle production vertex. Therefore, a value of P_{st} - average probability for a track to have a stereo confirmation of axial hits

$$P_{st} = N_{stereo}/N_{axial}$$

where N_{axial} is a number of axial hits found on a track and N_{stereo} is a number of stereo (SAS and Z) hits found in those layers, where track has axial hits, should be sensitive to correct hit assignment.

Distributions in P_{st} for the prompt and displaced CMUP muon tracks reconstructed in GHOST22 and JET50 samples are shown in the bottom row of Fig. 3. The GHOST22 and JET50 distributions in P_{st} are very similar and both, as expected, peak at 1 indicating that when a prompt track has an axial hit in a given silicon layer, in most cases in the same layer it also has a stereo silicon hit.

In contrast, distributions in P_{st} for the displaced tracks in both samples peak at $P_{st} = 0$. Peak at 0 means that axial and stereo hits associated with a track have been found in different layers, not confirming each other. Absense of the correlation between the axial and stereo silicon hits in a silicon detector with 2-sided readout can only be explained by a randomness of their assignment to a track.

This leads to a conclusion that displaced tracks with silicon hits and considered by CDF-9230 as passing loose SVX selection have their silicon hits misassigned which means that their large impact parameters are not confirmed by the SVX.

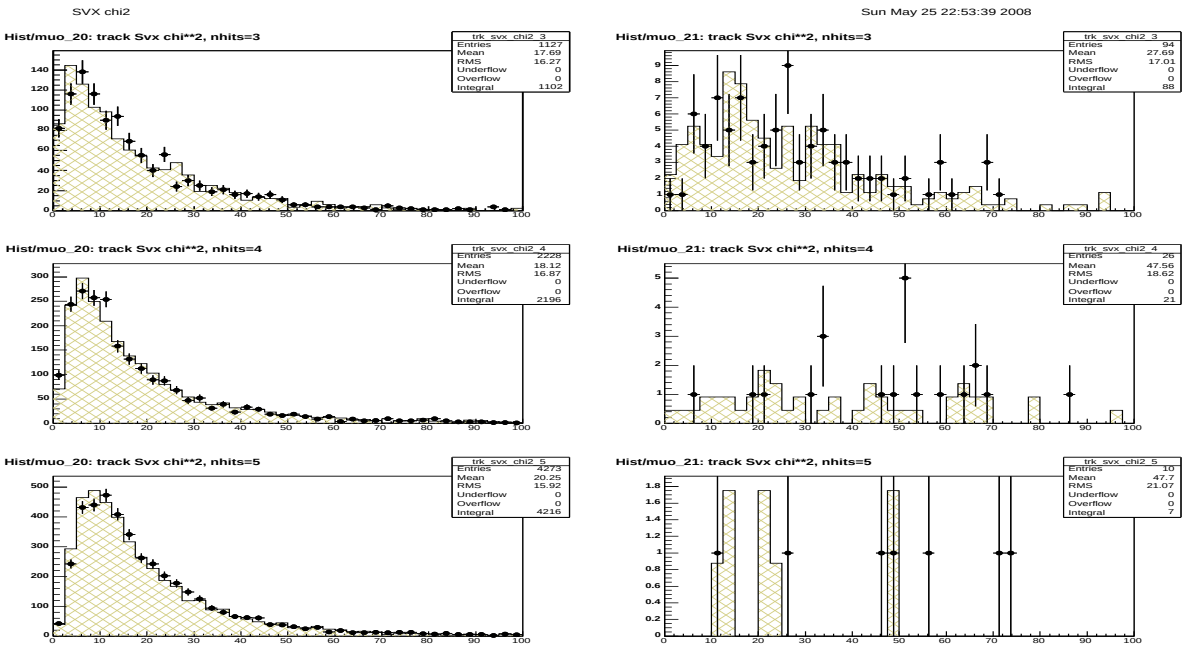

Figure 2: Distributions in χ^2_{SVX} for prompt (left histograms) and displaced (right histograms) tracks of reconstructed CMUP muons with different (3,4,5) number of axial SVX hits on a track. left: prompt tracks, right - displaced tracks
points with the error bars: GHOST22, histograms: JET50

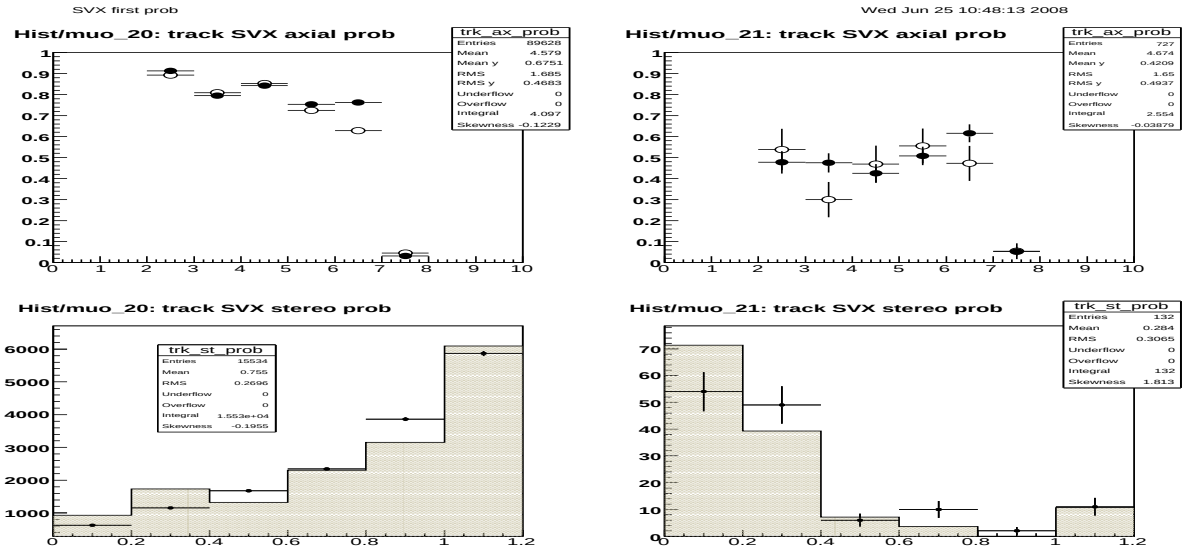

Figure 3: distributions in P_{ax} (top) and P_{st} (bottom) for tracks of CMUP muons reconstructed in JET50 and GHOST22 samples. left: muons with prompt tracks, right - muons with displaced tracks; filled points with the error bars: GHOST22, open points and histograms: JET50

3.2 COT tracking

Track reconstruction starts in COT, so the fact that displaced tracks do not have correct silicon hits may be a result of the COT track reconstruction. We therefore study quality of the COT tracks in GHOST22 sample and compare them to the COT tracks reconstructed in JET50 sample.

Fig. 4.top compares distributions χ^2_{COT}/DOF for tracks of prompt and displaced CMUP muons reconstructed in GHOST22 and JET50 samples. In both cases displaced COT tracks have average χ^2/DOF larger by about 20% than the prompt ones and the distributions for the location of the innermost COT track hit show that displaced tracks significantly more often, compared to the prompt tracks, don't have segments reconstructed in the inner COT superlayers. The feature is common for both GHOST22 and JET50 samples.

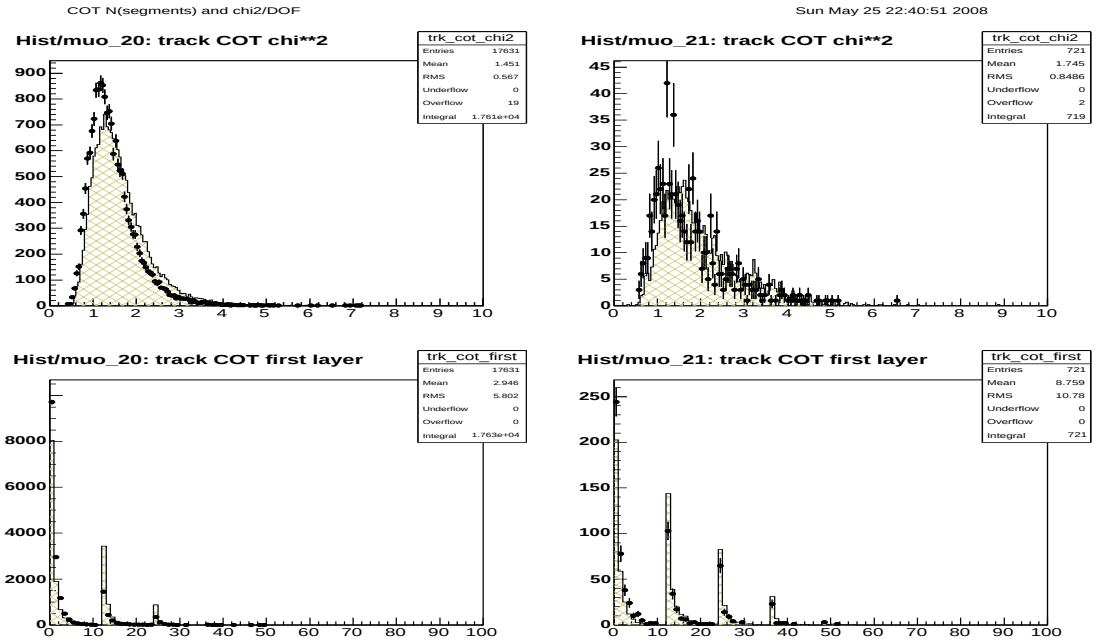

Figure 4: Distributions for χ^2_{COT}/DOF and location of the innermost COT hit for prompt (left histograms) and displaced (right histograms) tracks of CMUP muons. Points with the error bars: GHOST22, histograms: JET50.

3.3 Muons with large impact parameter : comparison to JET20 tracks

In order to understand origin of the long tails in the distributions for muon track impact parameter, d_0, - we compare distributions in d_0 for tracks of the muons reconstructed in GHOST22 sample to d_0 distributions of the tracks reconstructed in JET20 sample. JET20 track selection is fairly loose: a track is required to have

- $P_t > 2$GeV
- and at least 2 axial and 2 stereo COT segments with 5 hits per segment

No SVX-specific requirements are applied. Fig. 5 shows distributions in D0 for different GHOST22 muon categories (CMU/CMP/CMUP) overlaid with the D0 distribution for JET20 tracks, the same on all 3 plots.

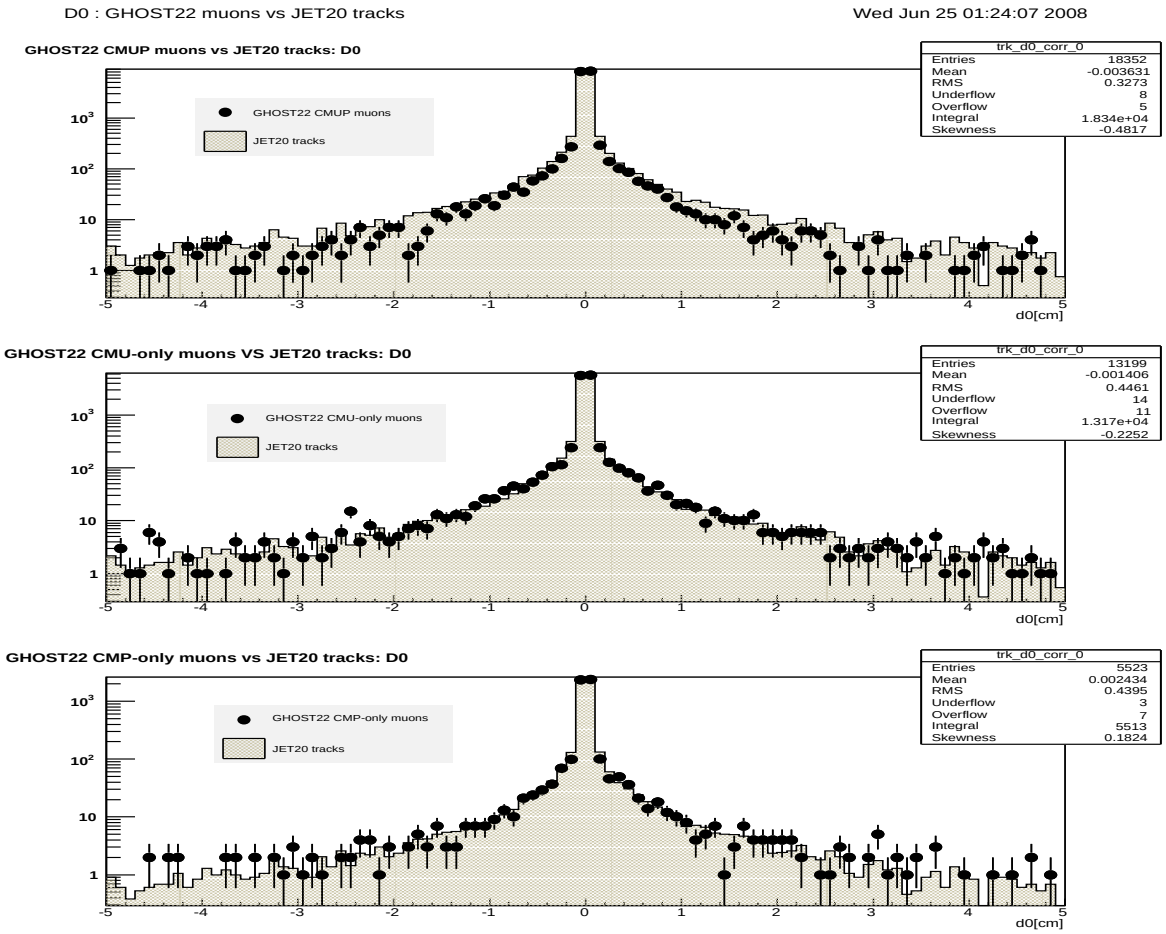

Figure 5: Distributions in impact parameter for different GHOST22 muon categories compared to JET20 tracks. Distributions normalized to the same area

D0 distributions for JET20 tracks shown in Fig. 5 also have very long tails which relatively are the same or higher than the corresponding tails in the distributions for GHOST22 muon tracks.

Although the underlying cause of the tails is yet to be understood, as JET20 trigger is prescaled by a factor of at least 240, we expect the tails in d_0 distributions for JET20 tracks to result from various detector and reconstruction effects: decays of the long-lived particles (K0s, lambda), secondary strong interactions in the tracker material, photon conversions, effects of the COT pattern recognition etc.

One could expect the same sources to contribute to the tails of the D0 distributions in GHOST22 sample as well, so any lifetime measurement with GHOST22 sample has to consider and subtract background coming from these sources.

We note that in the long lifetime-related part of the discussion of CDF-9230 these background sources are not taken into account.

4 Cross Checks of the Muon Reconstruction

In this section we check properties of muons reconstructed in GHOST22 multi-muon events and compare them to muons reconstructed in other data samples.

4.1 GHOST22 sample: CMU-only and CMP-only muons vs CMUP muons

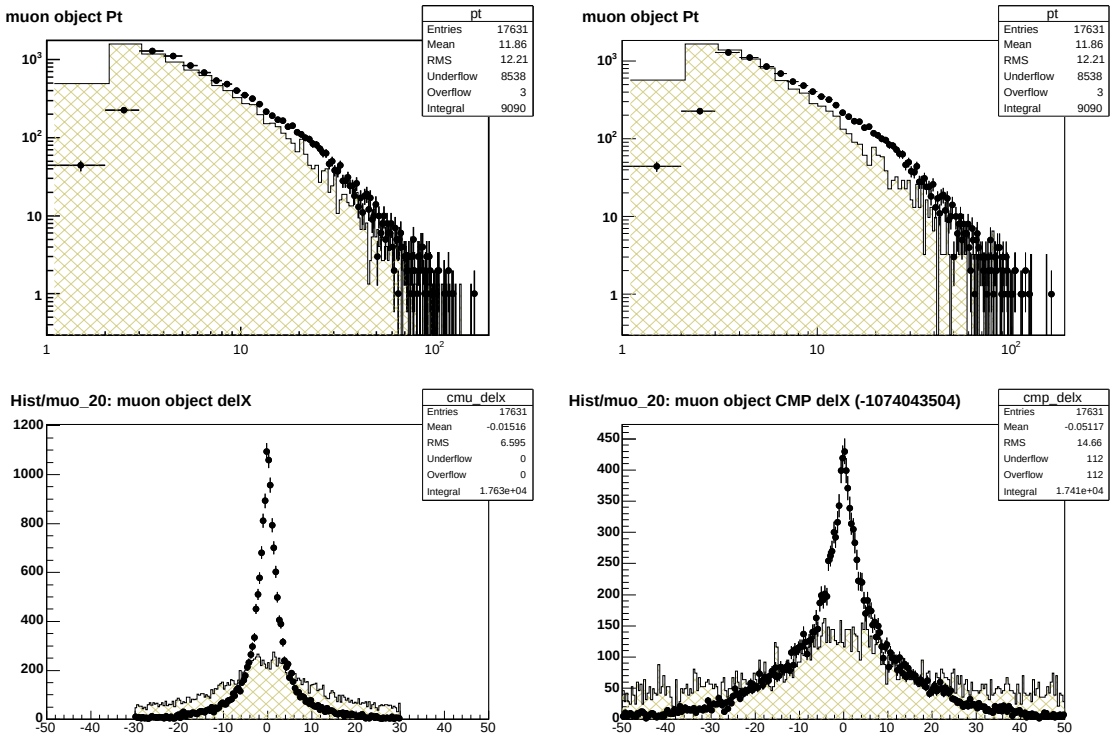

Figure 6: P_T spectra and ΔX distributions for CMUP, CMU-only and CMP-only muons in GHOST22 sample. left: Pt spectra of CMUP and CMU-only muons (top) and ΔX_{CMU} (bottom)
right: Pt spectra of CMUP and CMP-only muons (top) and ΔX_{CMP} (bottom)
In both cases points with the error bars correspond to CMUP muons

Along with CMUP muons analysis of CDF-9230 also uses CMU-only and CMP-only muons. Compared to the fist category, the last 2 muon categories usually have significantly lower purity. One of the ways estimate purity of the CMU-only and CMP-only muon samples is to compare them to CMUP muons.

Fig. 6.left_top compares momentum distributions for CMUP and CMU-only muons, the left_bottom distributions compares distributions in deltaX(CMU) for these 2 categories of muons.

Histograms on the right compare momentum distributions and distributions in deltaX(CMP) for CMUP and CMP-only muons.

Assuming that all the reconstructed CMUP muon objects are real muons and given that P_T spectra of CMUP and CMU-only muons are similar, we expect both categories of muons to have similar distributions in track-to-stub CMU rphi residuals. Based on similar arguments we also expect the distributions in CMP rphi residuals for CMUP and CMP-only muons to look similar.

The data look very different. As shown in Fig. 6, ΔX distributions for CMU-only and CMP-only muons are very different from the same distributions for CMUP muons. Even assuming that all the CMUP muons are real, is is very difficult to see how distributions in ΔX for CMU-only and CMP-only muons can accomodate non-negligible fraction of real muons.

4.2 Comparison between GHOST22 and J/psi muons

The fake muon candidate rate can be measured by analyzing the shape of muon matching variables such as the delta x and delta phi between the extrapolated track and the muon stub. These variables are compared between the 2-2 muon sample and a J/Psi sample with muon transverse momentums reweighed to match the 2-2 muon sample in Fig. 7. The delta x distribution is biased because in a dense environment the muon matching code may choose an incorrect stub that lies closer to the extrapolated track trajectory leading to a narrow component in the delta x distribution(fig 2). However, delta phi is not used in the reconstruction algorithm and is unbiased. Comparison of the shape of the delta phi distributions indicate that CMUP muon candidates in the 2-2 sample are at least 55% fake and CMP-only candidates are at least 75% fake(Fig. 8).

Note that the authors state that the expected fake rate in the CMUP is negligible.

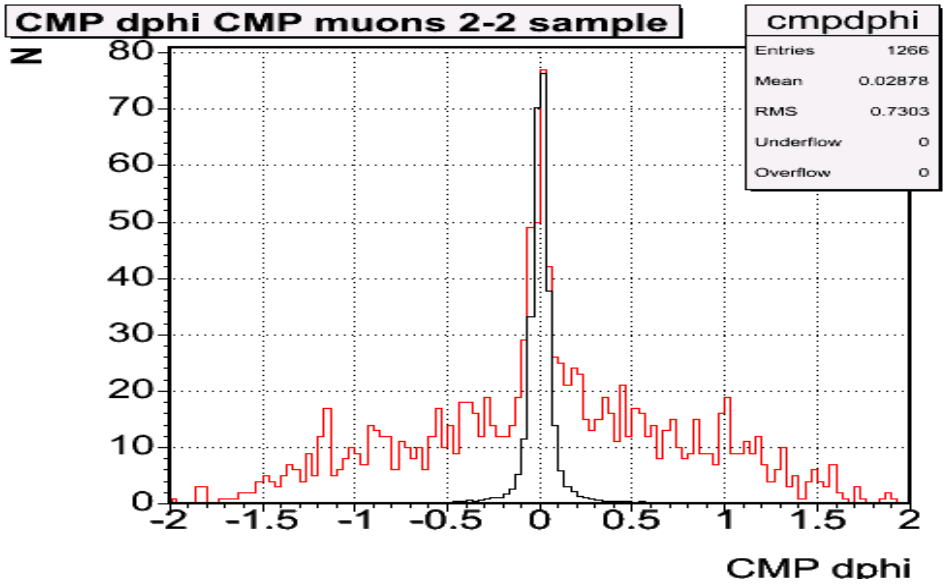

Figure 7:

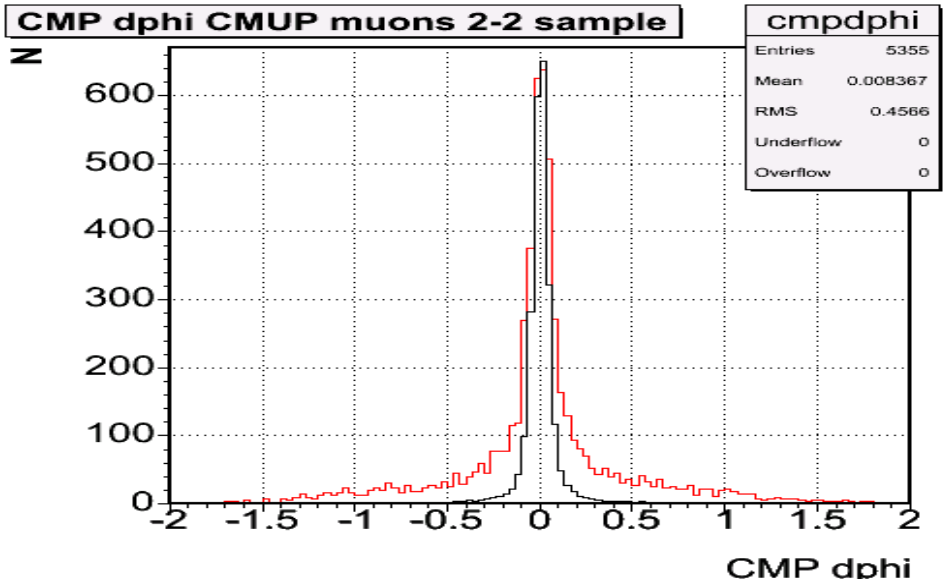

Figure 8:

4.3 Comparison between GHOST22 and JET50 muons

To complete study of the muon sample of CDF-9230 we compare GHOST22 muons to muons reconstructed in JET50 sample, where we expect the reconstructed muons to be predominantly fakes. Results of comparisons are presented in Fig. 9 and 10.

Fig. 9 compares distributions in muon track P_T and track-to-stub residuals for the CMUP muons reconstructed in JET50 and in GHOST22 samples. Average muon Pt in GHOST22 sample is about 30% higher than in JET50 sample, both ΔX_{CMU} and ΔX_{CMP} distribution for JET50 muons are about 30% wider and reweighting distributions in residuals to match the P_T spectra will result in very similar distributions. Therefore we conclude that distributions in RPHI residuals for CMUP muon objects reconstructed in GHOST22 and JET50 samples, taking into account difference in average Pt, look pretty much identical.

Next figure, Fig. 10 compares the same, Pt and $\Delta X_{CMU,CMP}$, distributions for CMU-only and CMP-only muons reconstructed in JET50 and in GHOST22 samples. Distributions in muon P_T for 2 samples are close enough to each other not distort distributions in ΔX.

CMU-only and CMP-only muons reconstructed in JET50 sample are expected to be primarily fakes, surprisingly, GHOST22 distributions look even less "muon-like" than the corresponding JET50 distributions. Overall the GHOST22 and JET20 distributions have similar widths, however, at small ΔX GHOST22 distributions, compared to JET50 distributions, are depleted.

In conclusion, we find that

- distributions for muon ID variables in GHOST22 sample are very different from what expected for the real muons with the same P_T spectrum;

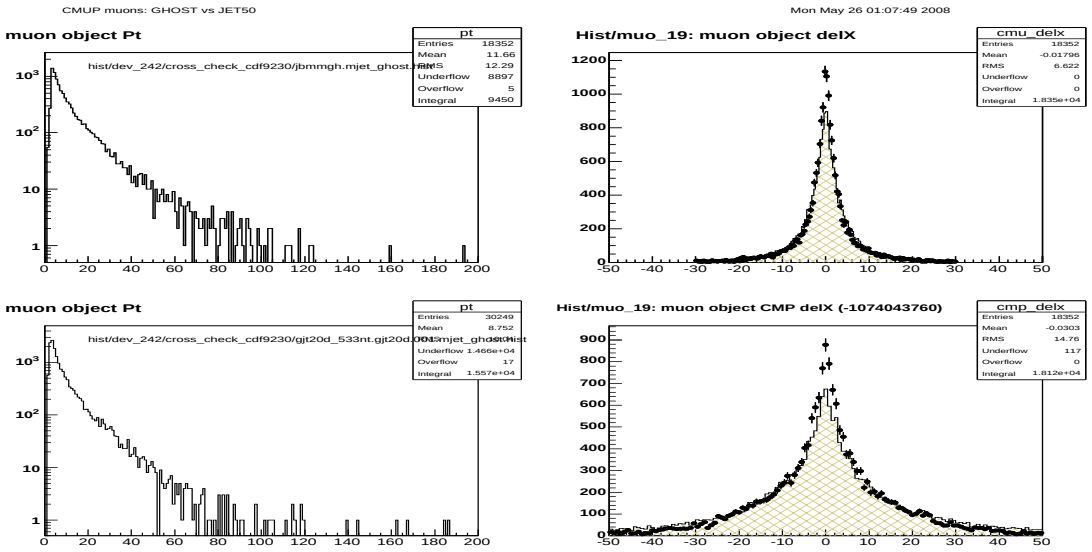

Figure 9: distributions for CMUP muons reconstructed in JET50 and GHOST22 samples
left: Pt distributions (top: GHOST22 sample, botom: JET50 sample).
right: distributions in track-to-sub residuals, top: DX(CMU), bottom: DX(CMP)
points with the error bars: JET50, histograms: GHOST22 sample
Average muon Pt in GHOST22 sample is about 30% higher than in JET50 sample which explains why JET50 residual distributions are about 30% wider.

- purity of the GHOST22 CMU-only and CMP-only muons is very low, possibly consistent with zero
- purity of GHOST22 CMUP muon sample is estimated to be below 50%
- distributions in rphi residuals for GHOST22 muons are very similar to the corresponding distributions for muons reconstructed in JET50 sample. We do not see any indication that purity of GHOST22 muons is higher than purity of JET50 muons.

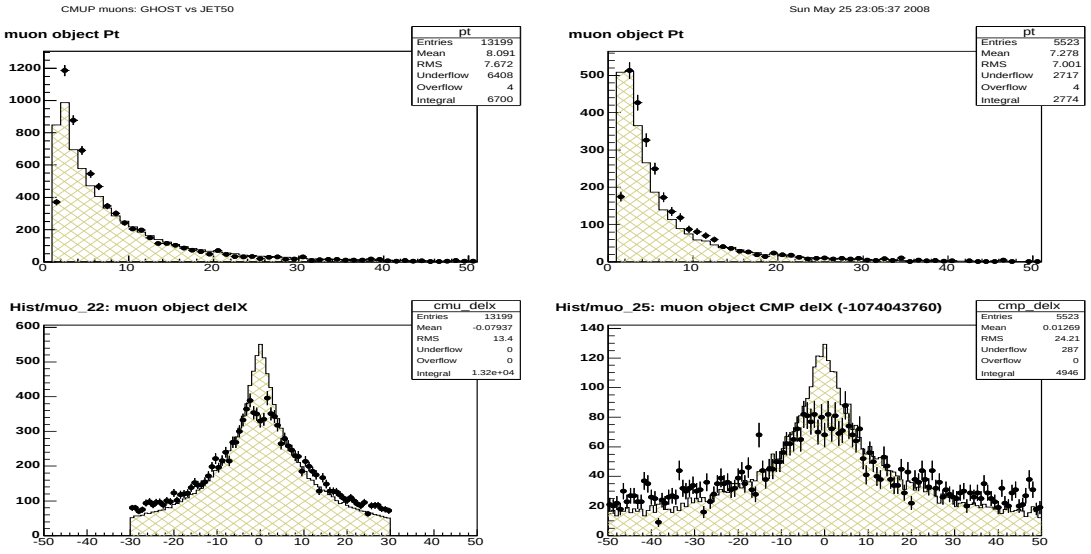

Figure 10: distributions for CMU-only and CMP-only muons reconstructed in JET50 and GHOST22 samples
points with the error bars: JET50, histograms: GHOST22 sample
left: CMU-only muons, right: CMP-only muons
top: Pt distributions, bottom: CMU or CMP DX distributions correspondingly

5 Jets in GHOST22 sample

Although selections used in CDF-9230 do not seem very different from selections of many other B-analyses, the selected analysis sample, and GHOST22 sample in particular, is very different from typical B-physics, low-pt, data samples.

Top-left plot in Fig. 11 shows distribution for the number of jets with $E_T > 20$ GeV reconstructed in GHOST22 sample. Distribution in number of jets peaks at N(jets)=2 and indicates that topology of GHOST22 events is very similar to QCD dijet events.

Shown in top-right plot of Fig. 11 distribution for the leading jet E_T has a very long tail - not only GHOST look like dijet events, these dijet events also have very energetic jets in them.

This observation points towards one more source of fake multi-muon events not considered by analysis of CDF-9230, namely "double-punchthrough" QCD events, dijet events with both jets leaking out of the calorimeter ang producing multiple hits in the muons chambers and thus firing the dimuon trigger.

The higher jet energy is, the higher is the probability for such a jet to generate a hadronic shower leaking out of the calorimeter and reaching the muon chambers. Using hits produced by the jet particles in the muon chambers, muon reconstruction code would reconstruct multiple muon stubs and link them to hadron tracks inside a jet, producing multiple "muons". In this case one would expect to see a very wide distribution in delta phi between a slope of the muon stub and a slope of the extrapolated track. Distribution in Fig. 7 is consistent with this expectation.

Event with fake muons reconstructed inside the jets penetrating the calorimeter and reaching the muon chambers should have the following features:

- probability to observe a fake muon in such an event is highly correlated with the probability to observe other muons nearby. Therefore punchthrough in high-Et jets is likely to have a high fraction of "multi-muon" events with "muons" going close to each other;

- probability for a given track inside a jet to become a fake muon is more likely to be a function of the total jet energy rather than of this track momentum: hits on a muon stub associated with the track to make a muon could be produced by a shower initiated by another, more energetic, charged particle or even a neutral particle inside this jet. So using fake rates parameterized versus track momentum could result in significant underestimate of the fake muon background.

In order to understand whether the jets in GHOST22 sample are different from generic QCD jets we select jets which have at least one reconstructed CMUP muon and one reconstructed CMU-only muon (to match preselections of GHOST22) and in the bottom plot in Fig. 11 compare average number of muons

$$\bar{N_\mu} =< N_{CMUP} + N_{CMU} + N_{CMP} >$$

reconstructed in cone=0.7 within the jet direction for jets in GHOST22, JET100, JET70 and JET50 samples. For this comparison we use "0I" jet datasets where JET70 and JET50 triggers was prescaled by a factor of 8. Because of the prescale any non-QCD physics source of muons would manifest itself as a differences between the JET50/JET70 and JET100 distributions in $\bar{N}_\mu(E_T)$.

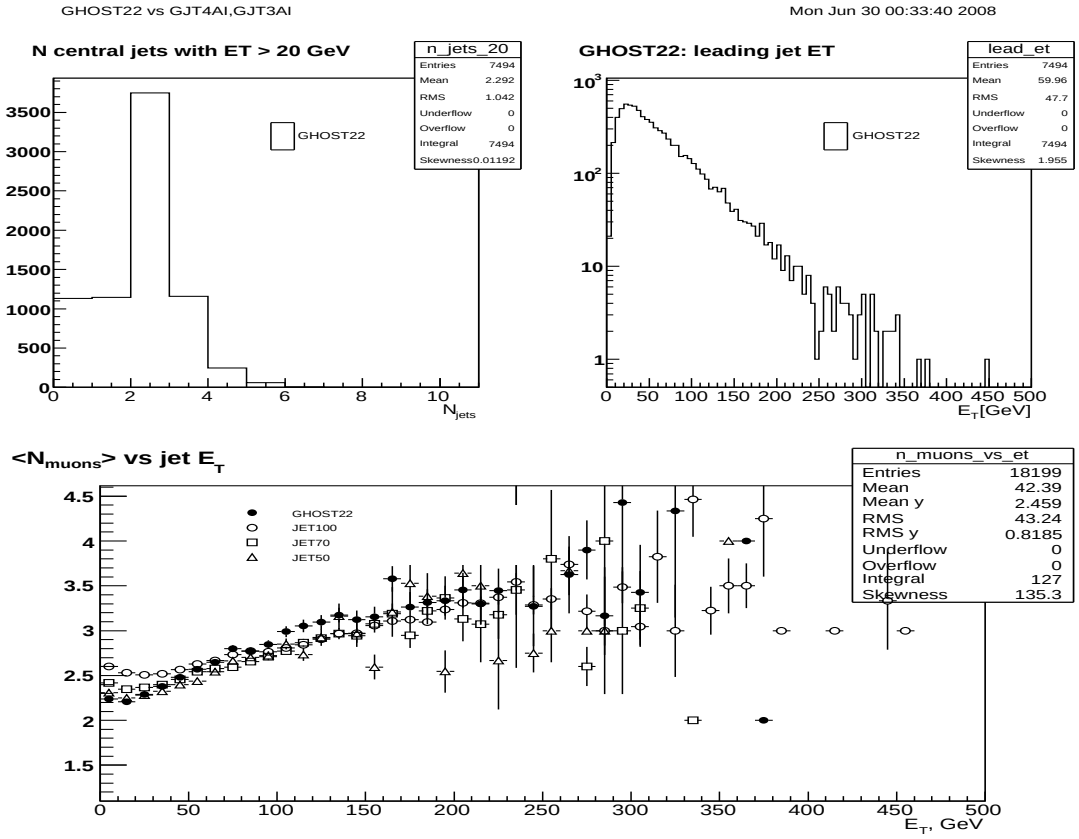

Figure 11: top-left: distributions in number of jets with E_T above 20 GeV in GHOST22 sample; top-right: E_T of the leading jet in GHOST22 sample; bottom: $\bar{N}_\mu(E_T)$vs jet E_T for JET50,JET70,JET100 and GHOST22 samples

We see that all 4 distributions $\bar{N}_\mu(E_T)$ agree with the accuracy better than 10% and do not find any evidence for additional source of muon production not consistent with high-Et jet punchthrough. It is interesting to note that for a 50 GeV generic jet with 1 CMUP and 1 CMU muons passing analysis cuts of CDF-9230 reconstructed in it, probability to find the 3rd muon passing the same cuts is about 50%. At about 150 GeV probability to find an additional, 3-rd, muon reaches 100%. Average E_T of the leading jet in GHOST22 sample is about 60GeV.

These observation together with the background subtraction method used in CDF-9230 allow to explain effects described there. There are several distinct types of events firing dimuon trigger:

- events with low-Pt muons, triggered by the real muons produced in heavy

flavor decays or fake muons from decays in flight etc

- events with high-Pt muons, triggered by Drell-Yan muons or muons from vector boson decays
- QCD events, triggered the fake muons reconstructed inside the jets punching through the calorimeter

Probability to have a misreconstructed track with artificially large impact parameter inside a high-Et jet is higher than in a low-density track environment. This is why long tails in d_0 distributions are not observed in J/phi sample shown on hte left plot in Fig. 12, while they are present in the J/psi sidebands - right plot in Fig. 12.

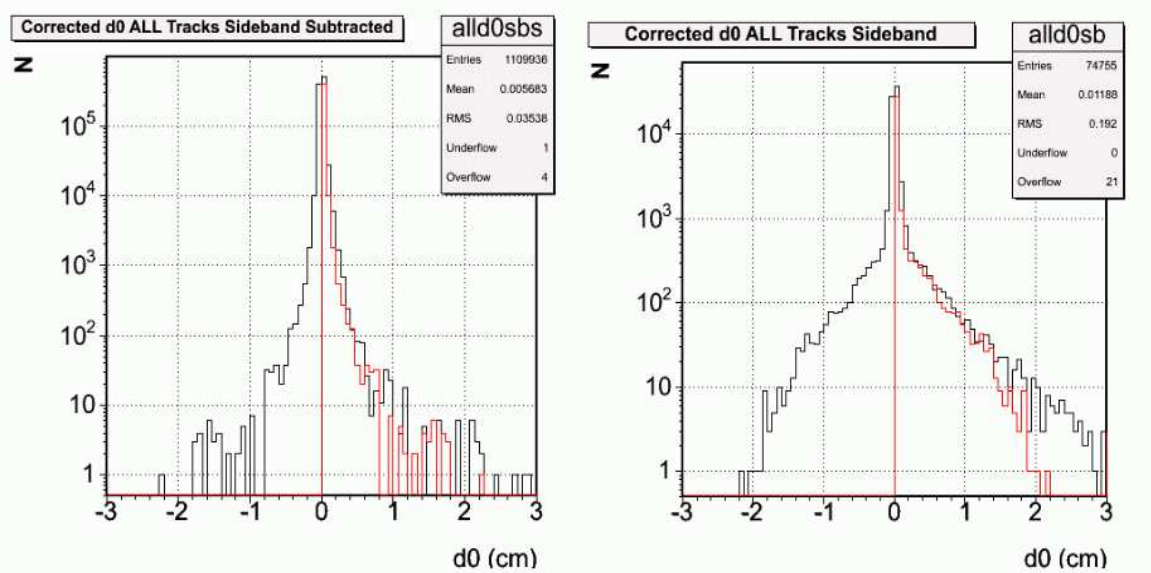

Figure 12: left plot: distribution in track signed impact parameter, $d_0 \cdot q_{track}$, for tracks of J/psi muons (sideband contribution subtracted)
right plot: distribution in $d_0 \cdot q_{track}$ for J/psi sidebands

Background subtraction used in CDF-9230, therefore, effectively subtracts first 2 sources of events and results in a sample enriched with high-Et QCD jet events which one could also expect to have other features pointed to in CDF-9230:

- high probability of punchthrough and thus multiple reconstructed (fake) muons
- high multiplicity of the tracks associated with the jets

We note that $\bar{N}_\mu(E_T)$distributions measured in generic QCD samples allow to predict absolute yield of multimuon events in GHOST22 sample.

To conclude, we find that GHOST22 events are predominantly events with high-Et jets and that $\bar{N}_\mu(E_T)$ for a jet with given E_T in GHOST22 sample is consistent

with the $\bar{N}_\mu(E_T)$ measured in JET100/JET70/JET50 samples. Yield of multimuon events in GHOST22 sample can therefore be explained based on the properties of generic QCD jets.

6 Conclusions

Having cross-checked analysis described in CDF-9230 we find that

- that silicon hits on the muon tracks with large impact parameters are predominantly misassigned. Therefore SVX-based background subtraction procedure used in CDF-9230 selects a sample enhanced in misreconstructed tracks
- long tails in muon track D0 distributions are observered not only in GHOST22 sample, but in JET50 and JET20 samples as well. Background sources resulting in the tails in JET50 and JET20 distributions are not taken into account by the analysis described in CDF-9230.
- samples of CMU-only and CMP-only muons in GHOST22 sample have very low, possibly consistent with 0, purity.
- comparison of GHOST22 CMUP muons to muons from J/psi decays indicates that purity of the GHOST22 CMUP muon sample is not higher than 50%.
- having compared muons reconstructed in GHOST22 sample to muons reconstructed in JET50 sample we didn't find indications that purity of GHOST22 muons is higher than purity of JET50 muons.
- most of GHOST22 events are high-Et jet events. Average number of muons, $\bar{N}_\mu(E_T)$, reconstructed within a jet of a given energy in GHOST22 sample is consistent with $\bar{N}_\mu(E_T)$ measured in JET100 and JET70 samples. Thus large yield of multimuon events in GHOST22 sample is not a surprize and could be expected based on the yield of fake muons measured in generic QCD samples.

References

[1] P.Giromini et al, Observation of anomalous multi-muon events produced in $p\bar{p}$ interactions at $\sqrt{s} = 1.96\ TeV$, CDF internal note 9230